Since January 2020 Elsevier has created a COVID-19 resource centre with free information in English and Mandarin on the novel coronavirus COVID-19. The COVID-19 resource centre is hosted on Elsevier Connect, the company's public news and information website.

Chemometrics and Intelligent Laboratory Systems 203 (2020) 104054

Contents lists available at ScienceDirect

Chemometrics and Intelligent Laboratory Systems

journal homepage: www.elsevier.com/locate/chemometrics

An automated Residual Exemplar Local Binary Pattern and iterative ReliefF based COVID-19 detection method using chest X-ray image

Turker Tuncer [a,*], Sengul Dogan [a], Fatih Ozyurt [b]

[a] Department of Digital Forensics Engineering, College of Technology, Firat University, Elazig, Turkey
[b] Department of Software Engineering, College of Engineering, Firat University, Elazig, Turkey

ARTICLE INFO

Keywords:
Residual Exemplar LBP
Covid-19
Iterative ReliefF
Classification
Machine learning

ABSTRACT

Coronavirus is normally transmitted from animal to person, but nowadays it is transmitted from person to person by changing its form. Covid-19 appeared as a very dangerous virus and unfortunately caused a worldwide pandemic disease. Radiology doctors use X-ray or CT images for the diagnosis of Covid-19. It has become crucial to help diagnose such images using image processing methods. Therefore, a novel intelligent computer vision method to automatically detect the Covid-19 virus was proposed. The proposed automatic Covid-19 detection method consists of preprocessing, feature extraction, and feature selection stages. Image resizing and grayscale conversion are used in the preprocessing phase. The proposed feature generation method is called Residual Exemplar Local Binary Pattern (ResExLBP). In the feature selection phase, a novel iterative ReliefF (IRF) based feature selection is used. Decision tree (DT), linear discriminant (LD), support vector machine (SVM), k nearest neighborhood (kNN), and subspace discriminant (SD) methods are chosen as classifiers in the classification phase. Leave one out cross-validation (LOOCV), 10-fold cross-validation, and holdout validation are used for training and testing. In this work, SVM classifier achieved 100.0% classification accuracy by using 10-fold cross-validation. This result clearly has shown that the perfect classification rate by using X-ray image for Covid-19 detection. The proposed ResExLBP and IRF based method is also cognitive, lightweight, and highly accurate.

1. Introduction

Coronavirus disease (Covid-19) is an infectious disease that occurs in Wuhan in December (2019) in China [1–3]. Covid-19 disease, which spreads from person to person rapidly all over the world, is a family of viruses capable of forming acute respiratory syndrome. The outer surface of the virus looks like spikes on the crown. Because of this structure, it is called coronavirus [4,5].

Diseases such as Severe Acute Respiratory Syndrome (SARS) and Middle East Respiratory Syndrome (MERS) can occur with this virus [6]. Thus, it causes acute lung damage and acute respiratory distress. This situation poses a serious risk to public health [7]. As 24 of March 2020; 382,057 people were infected worldwide and 16,565 of these cases resulted in death. The total infection rate was seen as 2.5% [8]. Given the mortality rates of all cases, Covid-19 appears to be the most threatening to the elderly population and those with chronic health problems [9]. This virus is transmitted from person to person through coughing, sneezing, respiratory droplets. This virus, which usually presents with symptoms of fever, cough, and shortness of breath, can have serious consequences such as pneumonia, multi-organ failure, and death [6,10]. Serious measures are taken to Covid-19 all over the world. Today, a clear solution has not been developed on Covid-19. The vast majority of measures taken on a country basis and individually are to prevent the transmission of this virus to more people. Thus, it is aimed to get time to produce solutions [11,12].

1.1. Motivation

Covid-19 is a world threatening virus and more than 300,000 people suffer from Covid-19. This disease is rapidly transmitted worldwide. In this study, a novel machine learning method to automatically detect this disease was presented. In infectious diseases, machine learning methods should be used in critical tasks. Therefore, our main motivation is to detect Covid-19 by using a computer vision method (without human).

1.2. Literature review

Studies on Covid-19 disease that appeared in December 2019 are

* Corresponding author.
E-mail addresses: turkertuncer@firat.edu.tr (T. Tuncer), sdogan@firat.edu.tr (S. Dogan), fatihozyurt@firat.edu.tr (F. Ozyurt).

https://doi.org/10.1016/j.chemolab.2020.104054
Received 25 March 2020; Received in revised form 1 May 2020; Accepted 12 May 2020
Available online 18 May 2020

a) Chest images diagnosed with Covid-19

b) Normal chest images

Fig. 1. Samples of the used Covid-19 and chest images.

limited. Many of these limited studies are for the recognition of the Covid-19 virus [13,14]. Also, some studies have been conducted on the effects of this disease on humans [15–19]. At the same time, the treatment of the Coronavirus and the processes occurring after it have been examined by Zhang et al. [2]. In the study, the possible conditions of the patient who was treated on Covid-19 disease and discharged were examined. Covid-19 was examined by Darlenski and Tsankov as dermatologists. They presented the effects of extreme hygiene measures on the skin and the factors that dermatologists will consider in this regard [20]. Chen et al. [21] focused on the prevent that can be taken for the Covid-19 virus and the success of a new type of treatment. The effect of mesenchymal stem cell therapy on the Covid-19 virus was interpreted with this study, and it was emphasized that it would be an alternative for treatment. Holland et al. [22] presented the kit developed by emergency doctors to protect against the Covid-19 virus. On the other hand, Yang et al. [23] examined the possible effects of the Covid-19 virus on children and their future. The study emphasized the importance of protection in children with other chronic conditions, and it was also emphasized that newborns should be isolated. Lai et al. [9] presented ways to protect against symptoms of coronavirus and pneumonia in their studies. In this study, it was found that it was mostly infected in adult patients. Li et al. [24] investigated the genetic evolution and source of the Covid-19 virus. These studies are currently limited in the literature and are expected to increase rapidly. However, symptoms of Covid-19 disease are similar to those of pneumonia, and a certain percentage of deaths due to the Covid-19 virus are on Pneumonia disease. There are many studies on the classification of Pneumonia disease with intelligent systems in the literature. Togacar et al. [25] have presented an intelligent classification system for Pneumonia disease. Chest X-ray images were used for this study. In the proposed study, deep learning methods were used and the results were presented by using AlexNet, VGG-16, and VGG-19 neural network models. The accuracy values for the selected dataset have resulted in 99.41%. Sousa et al. [26] provided automatic pneumonia diagnosis in infants through computer-aided systems from radiographic images. In this system, pneumonia data is classified using three classifiers. The classifiers used are Support Vector Machines, K-Nearest Neighbor, and Naïve Bayes. It was determined that the most suitable classifier for the available data is Support Vector Machines. Liang and Zheng [27] have developed a smart system for child Pneumonia disease. The convolutional neural network method was used in the developed system and the performance of Kermany [28] dataset was used. Classification accuracy was used as evaluation criteria. The accuracy value was calculated as 90.5% in the proposed method.

1.3. Our method

In this study, a novel method is presented to detect Covid-19 diagnosed. This method consists of preprocessing, feature extraction with Residual Exemplar Local Binary Pattern (ResExLBP), feature selection with iterative ReliefF (IRF), and classification phases. In the preprocessing phase, the input X-ray image is transformed into grayscale image and is resized 512×512 sized image. ResExLBP divides input image into 128×128 sized exemplars and LBP extracts feature from the input image and exemplars of it. The generated features are concatenated and discriminating ones of them are selected by using IRF. The selected features by IRF are utilized as input of the classifiers by using Leave one out cross-validation (LOOCV), 10-fold Cross Validation (CV), and holdout validation.

1.4. Contributions

The contributions of the proposed ResExLBP and IRF based Covid-19 detection method are given below.

- LBP is one of the widely used feature extractors in the literature and is effective method and generates high-level features. To achieve better classification rates and improve representation capability of the features, middle and low level features should be extracted like deep

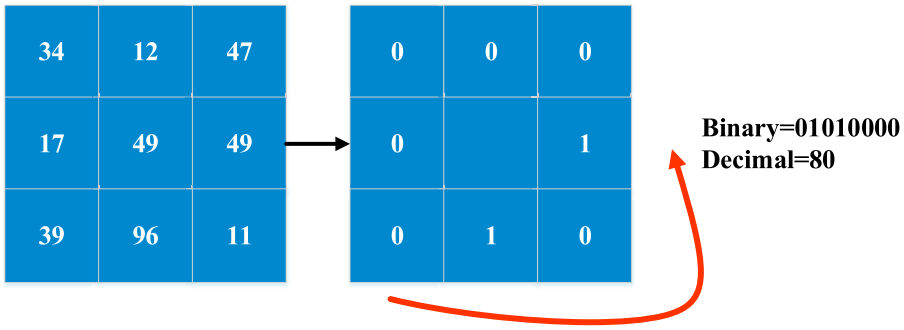

Fig. 2. Graphical explanation of the LBP.

networks. Therefore, ResExLBP is presented as a feature generation method. It uses both LBP and exemplar LBP together to extract low, middle, and high-level features. ReliefF is one of the most preferred distance based feature selector. It is a parametric feature selector. A new iterative ReliefF based feature selector (IRF) for automatic feature selection was presented.

- To obtain general performance, LOOCV, 10-fold CV, and holdout validation are used. Five classifiers were also selected to show the general success of the proposed ResExLBP and IRF based method. The proposed ResExLBP and IRF based method reached perfect classification rate (100.0%) for Covid-19 detection by using X-ray images.

2. Dataset

In this study, healthy and Covid-19 diagnosed images were used to assist the doctor in decision making on X-ray images. Public data were collected from the GitHub website [29]. 87 X-ray images with Covid-19 disease were collected. 26 of these patients are female and 41 are male and 20 of them are not determined. Patient ages are generally observed to be 50 and over. A total of 234 healthy X-ray chest images were obtained from the Kaggle site [30]. In order to increase the success of the proposed method, both the diagnosis of Covid-19 and healthy poster anterior (PA) images were selected. Example of the used chest images is given in Fig. 1.

3. Local binary pattern

LBP was presented in 1994 by Ojala. It is a very effective and simple feature extractor [31,32]. The main aim of the LBP is to extract local features for achieving global optimum features. Therefore, LBP divides the image into 3×3 sized overlapping blocks to extract neighborhood relations. The steps of the LBP are given below [33].

Step 0: Load input image with the size of W x H. W and H are the width and height of the image.
Step 1: Divide the input image into 3×3 sized overlapping block and obtain $(W-2)$ x $(H-2)$ blocks.
Step 2: Extract binary features from each block by using signum function. The description of the signum function is mathematically shown below.

$$bit(k) = signum(np, cp) = \begin{cases} 0, & np < cp \\ 1, & np \geq cp \end{cases}, \; k = \{1, 2, \ldots, 8\} \tag{1}$$

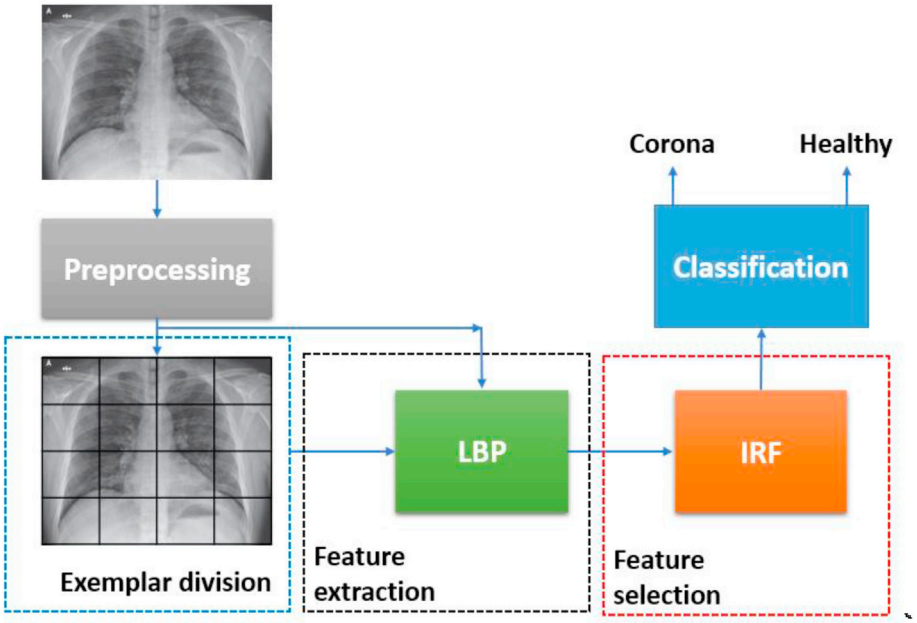

Fig. 3. Schematic demonstration of the proposed ResExLBP and IRF based method.

where *np* is a neighbor pixel, *cp* defines center pixel of the 3×3 sized block. In the 3×3 sized block, there are 8 neighbor pixels and a center pixel. Therefore, 8 bits are extracted from a pixel.

Step 3: Convert bits to a decimal value.

$$value(m,t) = \sum_{k=1}^{8} bit(k) * 2^{k-1},\ m = \{1,2,\ldots,W-2\},\ t = \{1,2,\ldots,H-2\} \quad (2)$$

Step 4: Construct a LBP implemented image by using values.
Step 5: Extract the histogram of the LBP implemented image. The extracted histogram is utilized as feature. LBP extracts 256 features because LBP implemented image is coded with 8-bit. A graphical explanation of the LBP is shown in Fig. 2 [34,35].

LBP is utilized as a basic feature in our feature generation model and LBP procedure was used for feature extraction. The pseudocode of the LBP is also shown in Algorithm 1 [36,37].

Algorithm 1. Pseudocode of LBP.

Procedure: Local binary pattern ($LBP(XI)$)
Input: X-ray image (XI) with size of W x H **Output:** Feature (feat) with size of 256.
00: Load XI 01: for i=1 to W-2 do 02: for j=1 to H-2 do 03: $block = XI(i{:}\,i+2, j{:}\,j+2)$; // 3 x 3 sized block division. 04: Use Eqs. 1-2 to calculate values. 05: end for j 06: end for i 07: Extract histogram of the value. // In here, the LBP image is coded as 8-bit. Therefore, the size of the histogram is calculated as $2^8 = 256$. This histogram is utilized as feature vector (feat)

4. The proposed X-ray image based automated Covid-19 detection method

An automated Covid-19 detection method by using novel feature generation model and an iterative feature selector was presented. Our feature generation model (ResExLBP) uses LBP and by using this model, 4352 features are extracted. To solve automatic feature selection of the ReliefF [38], an iterative model was presented. The selected most discriminating features are used as input of the classifiers. Our method consists of four main phases and these phases are shown in Fig. 3.

The used phases of the ResExLBP feature extraction and IRF feature selection based method are clearly explained in the subsection.

4.1. Preprocessing

The preprocessing phase is one of the most important phases of the proposed method because the success of this phase is directly affecting the classification capability. Here, basic and effective methods were used. The steps of this method are given below.

Step 0: Load raw X-ray image.
Step 1: Apply raw X-ray image to grayscale conversion.

$$gi = 0.3 * X - ray(:,:,1) + 0.59 * X - ray(:,:,2) + 0.11 * X - ray(:,:,3) \quad (3)$$

where $X - ray$ is three leveled image, gi expresses gray image.

Step 2: Resize grayscale image to 512×512 size image.

$$gi = resize(gi, 512\ \text{x}\ 512) \quad (4)$$

Step 3: Divide the image into 64×64 sized exemplars and obtain 64 exemplars.v

$$ex^t = gi(i : i+63, j : j+63),\ i = \{1,65,\ldots,449\},\ j = \{1,65,\ldots,449\},\ t = \{1,2,\ldots,64\} \quad (5)$$

In Eq. (5), ex^t expresses tth exemplar.

4.2. Residual exemplars local binary pattern based feature extraction: ResExLBP

In this phase, a novel feature extraction model which called ResExLBP is proposed. As we know from the literature, LBP is one of the effective feature extractions. The advantages of the LBP are given as follows. LBP extracts discriminative features, has low computational complexity, and application of it is easy because it has a basic algorithm. Because of these advantages, LBP was selected as feature extractor. The main problem of the LBP is to extract low-level features. Therefore, proposed residual and exemplar model extracts low, medium, and high-level features. The procedure of the ResExLBP is shown in Algorithm 2.

Algorithm 2. Pseudocode of the ResExLBP feature extraction method.

Input: Pre-processed image (*PI*) with size of 512 x 512.

Output: Features (*f*) with size of 256 x 17=4352

00: Load pre-processed image.
01: $cnt = 1$; // Counter defining
02: $f\left((cnt-1)*256+1{:}\,cnt*256\right) = LBP(PI)$;
03: $cnt++$;
04: **for** i=1 to 512 step by 64 **do**
05: **for** j=1 to 512 step by 64 **do**
06: $ex = PI(i{:}\,i+63, j{:}\,j+63)$; // Exemplars division
07: $f\left((cnt-1)*256+1{:}\,cnt*256\right) = LBP(ex)$; // Feature generation and concatenation.
08: $cnt++$;
09: **end for j**
10: **end for i**

In the ResExLBP, LBP is applied preprocessed image and 256 features are extracted from this image. Then, LBP is applied to exemplars of this image. 64 × 64 sized exemplars are used and 256 features each exemplar are generated. These features are concatenated and 4352 features are obtained. In the feature selection phase, most discriminating of the extracted 4352 features are selected.

4.3. Feature selection with iterative ReliefF

As we know from the literature, many feature reduction methods have been used to increase classification capability. ReliefF [38,39] is one of the distance based feature selectors in the literature. ReliefF uses Manhattan distance to calculate weights and generates both negative and positive weights. The negative weights assign redundant features in the ReliefF. ReliefF is an improved version of the Relief. In the Relief based feature selection method, Euclidean distance is used, but ReliefF uses Manhattan distance to generate weights. Mathematical notation of the ReliefF based weight generation is shown in Eqs. (6)–(8).

$$WR(ft_i) = WR(ft_i) - \frac{\sum_{j=1}^{k} dist(A,T,N)}{n*k} + \frac{\sum_{C\neq class(R)} \left[\frac{Pr(C)}{1-Pr(R)} * \sum_{l=1}^{k} dist(A,T,M)\right]}{n*k} \tag{6}$$

$$dist(A,L_1,L_2) = \begin{cases} 0, & L_1 = L_2 \\ 1, & L_1 \neq L_2 \end{cases} \tag{7}$$

$$dist(A,L_1,L_2) = \frac{|L_1 - L_2|}{A_{max} - A_{min}} \tag{8}$$

where $WR(ft_i)$ is weights of ith feature, k is missing number of classes, A is the vector of attributes, M is different class known as nearest miss, T is selected data in cycle, *dist* defines distance, N represents the nearest class, n is the number of cycles and Pr is probability.

One of the main problems of the ReliefF is to automatically select the most discriminating features. Therefore, an iterative ReliefF method is proposed. A loss calculator need to be selects for optimal features. Therefore, a classification method was used as loss value calculator and LD is chosen as loss calculator. The flow diagram of the proposed IRF is shown in Fig. 4.

The steps of the IRF are given below.

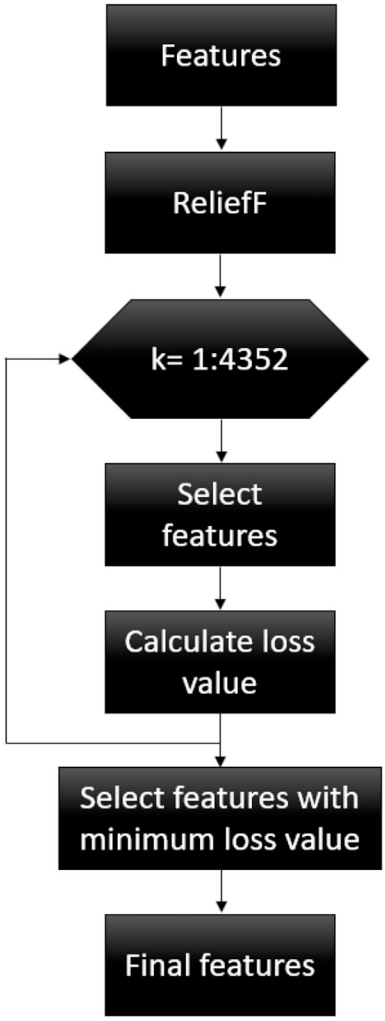

Fig. 4. Flow chart of the proposed IRF feature selector.

Table 1
Parameters of the used five classifiers.

Classifier	Parameter	Value
DT (Coarse Tree)	Splits	4
	Split method	Gini
	Decision of split	Off
LD	Covariance structure	Full
	Gamma	0
kNN (Fine kNN)	k	1
	Distance	City Block
	Weight	Equal
	Standardize	True
SVM (Medium Gaussian SVM)	Kernel function	Gaussian
	Kernel scale	38
	Number of box constraint	1
	Standardize	True
SD	Ensemble method	Subspace
	Number of learning cycles	30
	Learner	Discriminant
	Dimension	730

Step 1: Calculate ReliefF weights of the features.

$$w^R = ReliefF(f,\ target, 10) \tag{9}$$

where w^R is ReliefF weights and $ReliefF(.,.,.)$ is weight calculation function of the ReliefF.

Step 2: Sort w^R by descending to find indices of the sorted weights.

$$\left[w^R_{sorted}\ endex\right] = sort(w^R,\ descending) \tag{10}$$

where w^R_{sorted} sorted weights and *endex* is index of the positive weighted features.

Step 3: Calculate loss values of the features iteratively by using Algorithm 3.
Step 4: Find the minimum error.

$$[minimum\ indice] = min(loss) \tag{11}$$

where $min(.)$ is minimum function.

Step 5: Select optimum features by using *indice* and *endex* values.

$$feature(i) = f(endex(i)),\ i = \{1, 2, \ldots, indice\} \tag{12}$$

Algorithm 3. Loss values calculation procedure.

Input: Features ($\boldsymbol{f}$) with size of 4352 and ***endex*** with size of 4352, classifier (LDA) with 10-fold CV.

Output: Loss values (*loss*) with size of 4352.

```
00: Load features
01: for t=0 to 4351 do
02:     for i=1 to 1+t do
03:         feat(i) = f(endex(i));
04:     end for i
05:     loss(t) = LD(feat, 10); // Calculate loss value of the selected features by using LD classifier with 10-fold CV.
06: end for t
```

Table 2
Transitions of the proposed ResExLBP and IRF based.

	Step	Size	Size of feature
Preprocessing	Load chest image	W x H x 3	
	Grayscale conversion	W x H	
	Resizing	512 × 512	
Feature generation	Exemplar division	64 × 64 x 16	
	Feature generation from exemplars with LBP	64 × 64 x 16	256 × 16
	Feature generation from pre-processed image	512 × 512	256
	Feature fusion		256 × 17 = 4352
Feature selection with IRF	Most meaningful feature selection		1459
Classification	Classify the selected feature by 5 traditional classifiers	Validation prediction vector with the size of 321	

Table 3
Performance measurements (%) of the proposed ResExLBP and IRF based X-ray image classification method using LOOCV.

Classifier	CAC	SEN	SPE	BCAC	GM	Number of errors
DT	92.83	86.21	95.30	90.75	90.64	23
LD	99.07	96.55	100.0	98.28	98.26	3
kNN	97.20	89.66	100.0	94.83	94.69	9
SVM	99.69	98.85	100.0	99.43	99.42	1
SD	99.07	96.65	100.0	98.28	98.26	3

Steps 1–5 openly show the automatic feature selection process using ReliefF and LD. The LD classifier used in the Loss values calculation procedure is optional. The selected features by IRF are utilized as input of different classifiers. In this work, IRF selected 1459 features from the extracted 4352 features.

4.4. Classification

To show the effectiveness of the proposed ResExLBP and IRF based method, 5 classifiers were used. These classifiers are Decision tree (DT) [40,41], Linear Discriminant (LD) [42], k nearest neighborhood (kNN) [43], Support Vector Machines (SVM) [44] and subspace discriminant (SD) [45]. To show the general success of the proposed method, the optimal features were tested by using LOOCV, 10-fold CV, and holdout

validation. In the LOOCV, there is no random assignment. Therefore, it gives one accuracy value. 10-fold CV uses random selection, hence, it was executed 1000 times to evaluate general results. Two experimental studies were carried out in the Holdout validation section. The data were divided as 50% training, 50% test and 80% training, 20% test respectively. Then, again classifiers were executed 1000 times to evaluate general results. MATLAB Classification Learner (MCL) was used to execute these classifiers. Parameters of the used classifiers are shown in Table 1.

4.5. Overview of the proposed method

To clearly explain the proposed ResExLBP and IRF based chest image classification method, transitions of this method are shown in Table 2.

5. Results and discussions

Covid-19 causes chest viral infection and the proposed ResExLBP and IRF based method aimed to detect this viral infection. Therefore, a dataset from Kaggle and Github was collected. There are 321 chest X-ray images in this dataset. 87 of these X-ray images have belonged to Covid-19 and 234 of them have belonged to healthy subjects. In this section, our proposed method was tested on this dataset. This dataset is heterogeneous because there are 87 Covid-19 and 234 healthy subjects. If a classifier predicts all of them healthy, it achieved $234/321 = 72.89\%$ classification accuracy. Therefore, sensitivity, specificity, balanced accuracy, geometric mean, and accuracy evaluation criteria are used and the mathematical explanation of them is shown in Eqs. (13)–(17) [46–48].

$$CAC = \frac{TP + TN}{TP + TN + FP + FN} \tag{13}$$

$$SEN = \frac{TP}{TP + FN} \tag{14}$$

$$SPE = \frac{TN}{FP + TN} \tag{15}$$

$$BCAC = \frac{\left(\left(\frac{TP}{TP+FN}\right) + \left(\frac{TN}{FP+TN}\right)\right)}{2} \tag{16}$$

$$GM = \sqrt{\left(\frac{TP}{TP + FN}\right) \text{ x } \left(\frac{TN}{FP + TN}\right)} \tag{17}$$

where *TP*, *TN*, *FP*, and *FN* are true positive, true negative, false positive, and false negative respectively. *CAC* is classification accuracy, *SEN* represents sensitivity, *SPE* describes specificity, *BCAC* is balanced classification accuracy and *GM* denotes geometric mean.

LOOCV, 10-fold CV, and holdout validation methods are used for testing and training to obtain robust results. The obtained LOOCV results are listed in Table 3.

The calculated confusion matrices and ROC curves of the used classifiers with LOOCV are also shown in Fig. 5. To calculate general results by using 10-fold CV, classifiers were executed 1000 times and the obtained average, standard deviation, and maximum values were also shown in Table 4.

In LOOCV, there is no random selection for validation and testing.

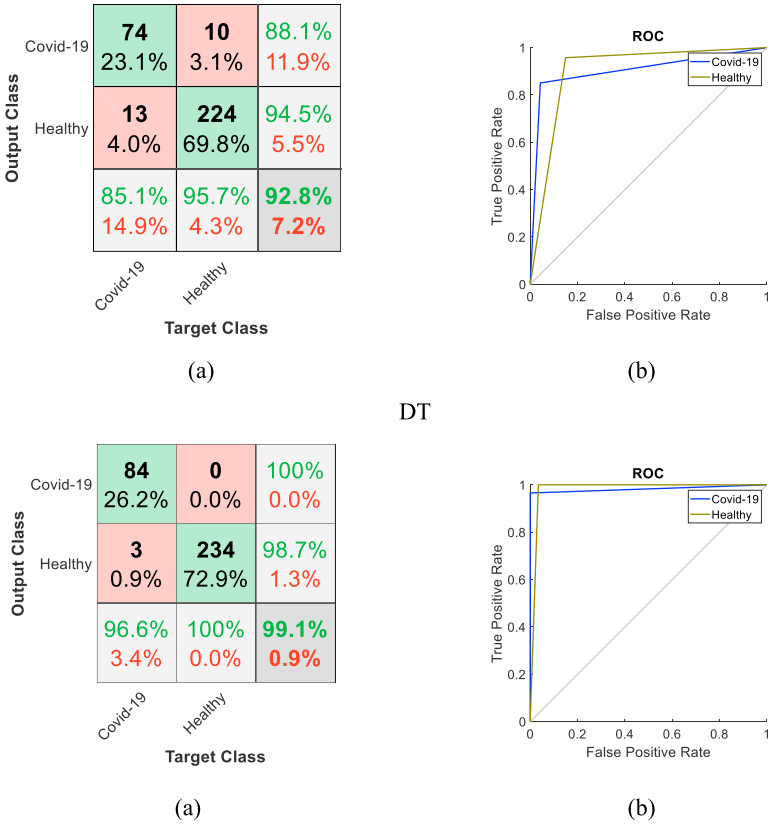

Fig. 5. LOOCV results of the proposed ResExLBP and IRF based Covid-19 detection method (a) Confusion matrix (b) ROC curve.

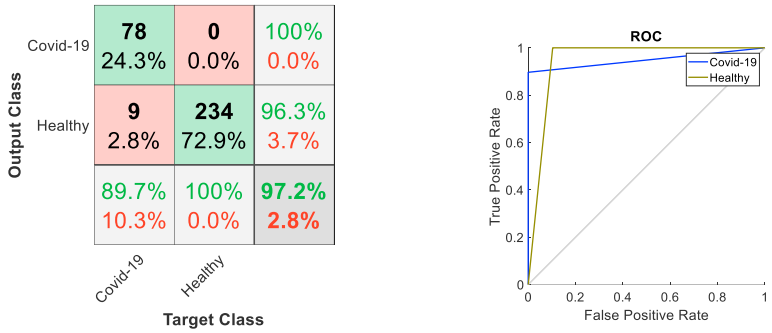

(a) (b)

kNN

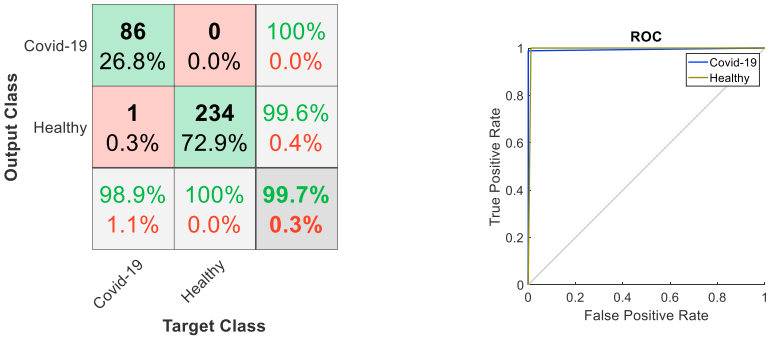

(a) (b)

SVM

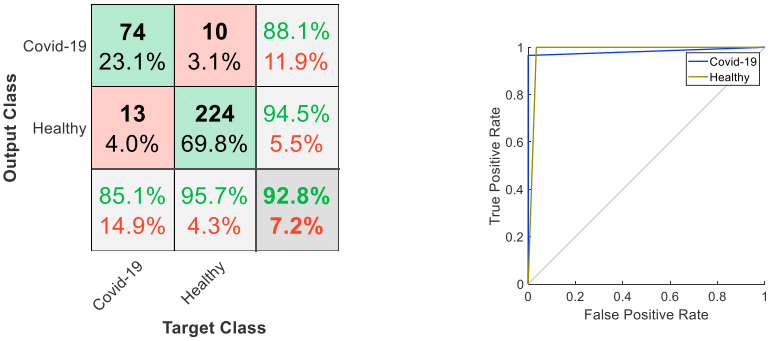

(a) (b)

SD

Fig. 5. (*continued*).

Therefore, there is no need to execute repeatedly.

To calculate holdout validation, data were divided as 80% training, 20% testing and 50% training, 50% testing. Classifiers were executed 1000 times and each obtained average, standard deviation, and maximum values were also shown in Tables 5 and 6.

As seen from Tables 4–6 SVM achieved 100.0% classification accuracy and the general success rate of the SVM was calculated above 99%. Tables 3–6 clearly show that the best classifier is SVM and the worst resulted classifier is DT. SD and LD achieved the same success rates by using LOOCV and holdout validation. However, LD reached a higher success rate than SD by using 10-fold CV and holdout validations. The scatter plot of the extracted features is presented in Fig. 6.

Fig. 6 shows the success of the proposed ResExLBP and IRF clearly. In this figure, only scatter plot of the first and second features is shown. Advantages of the proposed ResExLBP and IRF based method are;

Table 4
Performance measurements (%) of the proposed ResExLBP and IRF based X-ray image classification method using the 10-fold CV.

Classifier	Statistics	CAC	SEN	SPE	BCAC	GM
DT	Mean	96.63	87.55	100.0	93.78	93.56
	Std	0.53	1.95	0.0	0.97	1.05
	Max	97.82	91.95	100.0	95.98	95.89
LD	Mean	99.11	95.81	99.97	97.89	97.87
	Std	0.44	1.18	0.11	0.59	0.60
	Max	99.69	98.85	100.0	99.43	99.42
kNN	Mean	96.63	87.55	100.0	93.78	93.56
	Std	0.53	1.95	0	0.97	1.05
	Max	97.82	91.95	100.0	95.98	95.89
SVM	Mean	99.55	98.29	100.0	99.15	99.14
	Std	0.17	0.59	0	0.30	0.30
	Max	100.0	100.0	100.0	100.0	100.0
SD	Mean	98.70	94.89	100.0	97.45	97.41
	Std	0.47	1.44	0	0.72	0.74
	Max	99.07	96.55	100.0	98.28	98.26

Table 5
Performance measurements (%) of the proposed ResExLBP and IRF based X-ray image classification method using the 80% training, 20% testing.

Classifier	Statistics	CAC	SEN	SPE	BCAC	GM
DT	Mean	91.30	82.97	94.44	88.71	88.35
	Std	3.5	9.18	3.8	4.7	5.10
	Max	100.0	100.0	100.0	100	100.0
LD	Mean	98.61	95.05	99.95	97.50	97.43
	Std	1.40	5.07	0.34	2.54	2.64
	Max	100.0	100.0	100.0	100.0	100.0
kNN	Mean	96.62	87.64	100.0	93.82	93.52
	Std	2.09	7.65	0	3.83	4.17
	Max	100.0	100.0	100.0	100.0	100.0
SVM	Mean	99.45	97.98	100.0	98.99	98.97
	Std	0.85	3.09	0	1.54	1.58
	Max	100.0	100.0	100.0	100.0	100.0
SD	Mean	98.09	93.04	99.9	96.52	96.40
	Std	1.67	6.09	0.001	3.04	3.21
	Max	100.0	100.0	100.0	100.0	100.0

Table 6
Performance measurements (%) of the proposed ResExLBP and IRF based X-ray image classification method using the 50% training, 50% testing.

Classifier	Statistics	CAC	SEN	SPE	BCAC	GM
DT	Mean	90.49	81.49	93.8	87.64	87.32
	Std	2.4	7.06	2.83	3.43	3.73
	Max	95.63	100.0	100.0	94.99	94.95
LD	Mean	97.74	91.80	99.93	95.86	95.75
	Std	1.14	4.23	0.24	2.11	2.22
	Max	100.0	100.0	100.0	100.0	100.0
kNN	Mean	95.39	82.84	100.0	91.42	90.96
	Std	1.64	6.08	0	3.04	3.38
	Max	99.38	97.67	100.0	98.84	98.83
SVM	Mean	99.06	96.63	99.95	98.29	98.26
	Std	0.89	3.32	0.20	1.65	1.70
	Max	100.0	100.0	100.0	100.0	100.0
SD	Mean	96.84	88.48	99.91	94.14	93.99
	Std	1.30	4.79	0.30	2.39	2.56
	Max	100.0	100.0	100.0	100.0	100.0

- ResExLBP increased the feature extraction capability of the LBP. Because LBP extracts low-level feature but our proposed ResExLBP extracts low, medium and high-level features.
- The automatic feature selection problem of the ReliefF is solved by proposing IRF.
- A novel automated Covid-19 detection method with high accuracy was presented.

6. Conclusions and suggestions

In this paper, a novel method to accurately detect Covid-19 patients by using chest X-ray images was presented. The proposed hybrid method is ResExLBP feature extraction and IRF feature selection methods. The main objective of the ResExLBP is to extract meaningful features and IRF is proposed to select the most discriminative features. The selected most discriminative features were classified by 5 classifiers with LOOCV, 10-fold CV, and holdout validation methods. The proposed ResExLBP and IRF based method achieved 99.69% and 100.0% classification accuracy by using SVM with LOOCV and 10-fold CV respectively.

7. Future directions

Future studies on the proposed method are given below.

- Covid-19 is a deadly virus and it has been seen worldwide. Smart health systems should be used to detect Covid-19 quickly. A novel smart heath assistant can be developed by using the proposed ResExLBP and IRF together. A proposal for these smart assistants is illustrated in Fig. 7.
- Quarantine is one of the applied effective methods to prevent the spread of the coronavirus (Covid-19). It is very important to establish unmanned health units to track patients in quarantine and protect health workers. In these units, intelligent systems can be used to track patients and these systems can be developed by using machine learning method as the proposed ResExLBP and IRF based method.
- In this proposed method, Residual Exemplar Local Binary Pattern (ResExLBP) was used as feature extractor. Researchers can be used other feature extractors in the residual exemplar model and they can propose novel ResEx based methods.
- The proposed model can be used as a solution method to solve other biomedical image problems.

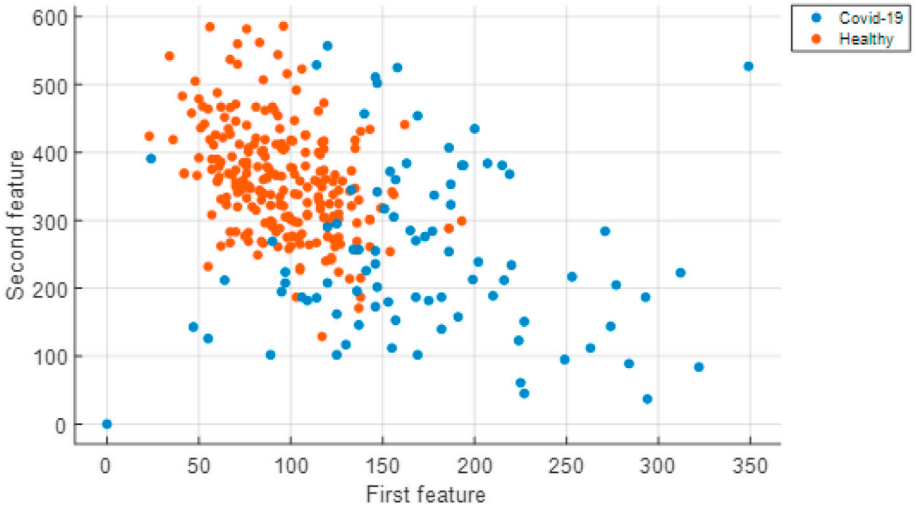

Fig. 6. Scatter plot of the extracted and selected features.

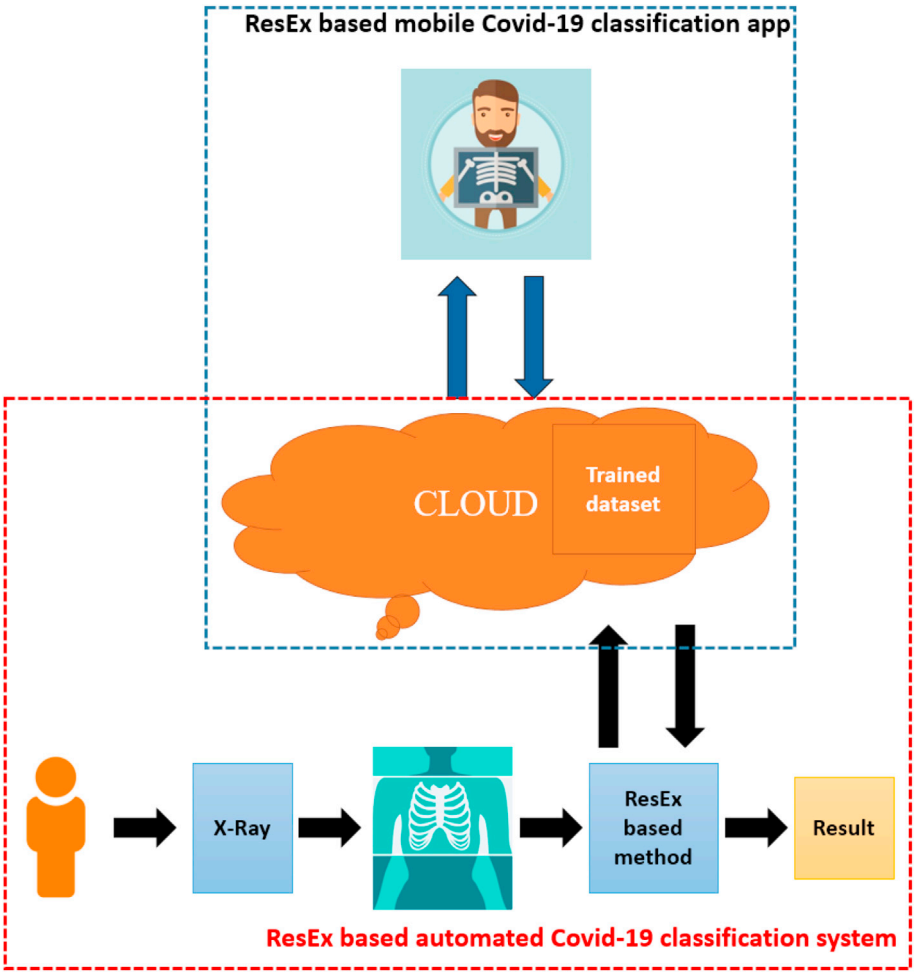

Fig. 7. Future applications about Covid-19 detection.

Declaration of competing interest

There is no Conflict of Interest.

CRediT authorship contribution statement

Turker Tuncer: Conceptualization, Formal analysis, Writing - original draft, Writing - review & editing. **Sengul Dogan:** Conceptualization, Formal analysis, Writing - original draft, Writing - review & editing. **Fatih Ozyurt:** Funding acquisition, Formal analysis, Writing - review & editing.

References

[1] H. Lau, V. Khosrawipour, P. Kocbach, A. Mikolajczyk, H. Ichii, J. Schubert, J. Bania, T. Khosrawipour, Internationally lost COVID-19 cases, J. Microbiol. Immunol. Infect. (2020).
[2] J.-f. Zhang, K. Yan, H.-h. Ye, J. Lin, J.-j. Zheng, T. Cai, SARS-CoV-2 turned positive in a discharged patient with COVID-19 arouses concern regarding the present standard for discharge, Int. J. Infect. Dis. (2020).
[3] G. Lippi, M. Plebani, B.M. Henry, Thrombocytopenia is associated with severe coronavirus disease 2019 (COVID-19) infections: a meta-analysis, Clin. Chim. Acta (2020).
[4] H.A. Rothan, S.N. Byrareddy, The epidemiology and pathogenesis of coronavirus disease (COVID-19) outbreak, J. Autoimmun. (2020) 102433.
[5] S. Chavez, B. Long, A. Koyfman, S.Y. Liang, Coronavirus Disease (COVID-19): a primer for emergency physicians, Am. J. Emerg. Med. (2020).
[6] A.J. Rodriguez-Morales, J.A. Cardona-Ospina, E. Gutiérrez-Ocampo, R. Villamizar-Peña, Y. Holguin-Rivera, J.P. Escalera-Antezana, L.E. Alvarado-Arnez, D.K. Bonilla-Aldana, C. Franco-Paredes, A.F. Henao-Martinez, Clinical, laboratory and imaging features of COVID-19: a systematic review and meta-analysis, Trav. Med. Infect. Dis. (2020) 101623.
[7] A. Cortegiani, G. Ingoglia, M. Ippolito, A. Giarratano, S. Einav, A systematic review on the efficacy and safety of chloroquine for the treatment of COVID-19, J. Crit. Care (2020).
[8] https://www.statista.com/topics/5994/the-coronavirus-disease-covid-19-outbreak/.
[9] C.-C. Lai, Y.H. Liu, C.-Y. Wang, Y.-H. Wang, S.-C. Hsueh, M.-Y. Yen, W.-C. Ko, P.-R. Hsueh, Asymptomatic carrier state, acute respiratory disease, and pneumonia due to severe acute respiratory syndrome coronavirus 2 (SARSCoV-2): facts and myths, J. Microbiol. Immunol. Infect. (2020).
[10] C. Sohrabi, Z. Alsafi, N. O'Neill, M. Khan, A. Kerwan, A. Al-Jabir, C. Iosifidis, R. Agha, World Health Organization declares global emergency, A review of the 2019 novel coronavirus (COVID-19), Int. J. Surg. (2020).
[11] L.-s. Wang, Y.-r. Wang, D.-w. Ye, Q.-q. Liu, A review of the 2019 Novel Coronavirus (COVID-19) based on current evidence, Int. J. Antimicrob. Agents (2020) 105948.
[12] J. Yang, Y. Zheng, X. Gou, K. Pu, Z. Chen, Q. Guo, R. Ji, H. Wang, Y. Wang, Y. Zhou, Prevalence of comorbidities in the novel Wuhan coronavirus (COVID-19) infection: a systematic review and meta-analysis, Int. J. Infect. Dis. (2020).
[13] M.A. Shereen, S. Khan, A. Kazmi, N. Bashir, R. Siddique, COVID-19 infection: origin, transmission, and characteristics of human coronaviruses, J. Adv. Res. (2020).
[14] K. Mizumoto, G. Chowell, Transmission potential of the novel coronavirus (COVID-19) onboard the diamond princess Cruises ship, Infect. Dis. Model. (2020), 2020.
[15] Z. Li, J. Ge, M. Yang, J. Feng, M. Qiao, R. Jiang, J. Bi, G. Zhan, X. Xu, L. Wang, Vicarious traumatization in the general public, members, and non-members of medical teams aiding in COVID-19 control, Brain Behav. Immun. (2020).
[16] N. Liu, F. Zhang, C. Wei, Y. Jia, Z. Shang, L. Sun, L. Wu, Z. Sun, Y. Zhou, Y. Wang, Prevalence and predictors of PTSS during COVID-19 outbreak in China hardest-hit areas: gender differences matter, Psychiatr. Res. (2020) 112921.
[17] T.R. Wind, M. Rijkeboer, G. Andersson, H. Riper, The COVID-19 Pandemic: the 'black Swan' for Mental Health Care and a Turning Point for E-Health, Elsevier, 2020.
[18] D. Banerjee, The COVID-19 outbreak: crucial role the psychiatrists can play, Asian J. Psychiatr. (2020) 102014.
[19] Y. Yang, W. Li, Q. Zhang, L. Zhang, T. Cheung, Y.-T. Xiang, Mental health services for older adults in China during the COVID-19 outbreak, Lancet Psychiatr. 7 (2020) e19.

[20] R. Darlenski, N. Tsankov, Covid-19 pandemic and the skin - what should dermatologists know? Clin. Dermatol. (2020).
[21] J. Chen, C. Hu, L. Chen, L. Tang, Y. Zhu, X. Xu, L. Chen, H. Gao, X. Lu, L. Yu, Clinical study of mesenchymal stem cell treating acute respiratory distress syndrome induced by epidemic Influenza A (H7N9) infection, a hint for COVID-19 treatment, Engineering (2020).
[22] M. Holland, D.J. Zaloga, C.S. Friderici, COVID-19 personal protective equipment (PPE) for the emergency physician, Visual J. Emerg. Med. 19 (2020) 100740.
[23] P. Yang, P. Liu, D. Li, D. Zhao, Corona Virus Disease 2019, a growing threat to children? J. Infect. (2020).
[24] C. Li, Y. Yang, L. Ren, Genetic evolution analysis of 2019 novel coronavirus and coronavirus from other species, Infect. Genet. Evol. (2020) 104285.
[25] M. Toğaçar, B. Ergen, Z. Cömert, A Deep Feature Learning Model for Pneumonia Detection Applying a Combination of mRMR Feature Selection and Machine Learning Models, IRBM, 2019.
[26] R.T. Sousa, O. Marques, F.A.A. Soares, I.I. Sene Jr., L.L. de Oliveira, E.S. Spoto, Comparative performance analysis of machine learning classifiers in detection of childhood pneumonia using chest radiographs, Procedia Comput. Sci. 18 (2013) 2579–2582.
[27] G. Liang, L. Zheng, A Transfer Learning Method with Deep Residual Network for Pediatric Pneumonia Diagnosis, Computer Methods and Programs in Biomedicine, 2019, p. 104964.
[28] D. Kermany, K. Zhang, M. Goldbaum, Labeled optical coherence tomography (oct) and chest X-ray images for classification, 2, Mendeley data, 2018.
[29] Github. https://github.com/, 2020.
[30] Kaggle. https://www.kaggle.com/, 2020.
[31] T. Ojala, M. Pietikainen, D. Harwood, Performance evaluation of texture measures with classification based on Kullback discrimination of distributions, in: Proceedings of 12th International Conference on Pattern Recognition, IEEE, 1994, pp. 582–585.
[32] M. Pietikaeinen, T. Ojala, J. Nisula, J. Heikkinen, Experiments with two industrial problems using texture classification based on feature distributions, in: Intelligent Robots and Computer Vision XIII: 3D Vision, Product Inspection, and Active Vision, International Society for Optics and Photonics, 1994, pp. 197–204.
[33] T. Ojala, M. Pietikäinen, T. Mäenpää, A generalized local binary pattern operator for multiresolution gray scale and rotation invariant texture classification, in: International Conference on Advances in Pattern Recognition, Springer, 2001, pp. 399–408.
[34] T. Ahonen, A. Hadid, M. Pietikäinen, Face Recognition with Local Binary Patterns, European Conference on Computer Vision, Springer, 2004, pp. 469–481.
[35] M. Pietikäinen, Local binary patterns, Scholarpedia 5 (2010) 9775.
[36] T. Tuncer, S. Dogan, F. Ertam, Automatic voice based disease detection method using one dimensional local binary pattern feature extraction network, Appl. Acoust. 155 (2019) 500–506.
[37] T. Tuncer, S. Dogan, Pyramid and multi kernel based local binary pattern for texture recognition, J. Ambient Intell. Humanized Comput. 11 (2020) 1241–1252.
[38] M. Robnik-Šikonja, I. Kononenko, Theoretical and empirical analysis of ReliefF and RReliefF, Mach. Learn. 53 (2003) 23–69.
[39] S. Demir, S. Key, T. Tuncer, S. Dogan, An exemplar pyramid feature extraction based humerus fracture classification method, Med. Hypotheses (2020) 109663.
[40] S.R. Safavian, D. Landgrebe, A survey of decision tree classifier methodology, IEEE Trans. Syst. Man Cybern. 21 (1991) 660–674.
[41] K. Polat, S. Güneş, Classification of epileptiform EEG using a hybrid system based on decision tree classifier and fast Fourier transform, Appl. Math. Comput. 187 (2007) 1017–1026.
[42] S. Chen, X. Yang, Alternative linear discriminant classifier, Pattern Recogn. 37 (2004) 1545–1547.
[43] Q. Hu, D. Yu, Z. Xie, Neighborhood classifiers, Expert Syst. Appl. 34 (2008) 866–876.
[44] K. Lau, Q. Wu, Online training of support vector classifier, Pattern Recogn. 36 (2003) 1913–1920.
[45] Y. Zhu, S. Schwartz, M. Orchard, Fast face detection using subspace discriminant wavelet features, in: Proceedings IEEE Conference on Computer Vision and Pattern Recognition. CVPR 2000 (Cat. No. PR00662), IEEE, 2000, pp. 636–642.
[46] T. Tuncer, S. Dogan, P. Pławiak, U.R. Acharya, Automated arrhythmia detection using novel hexadecimal local pattern and multilevel wavelet transform with ECG signals, Knowl. Base Syst. 186 (2019) 104923.
[47] T. Tuncer, F. Ertam, S. Dogan, E. Aydemir, P. Pławiak, Ensemble residual network-based gender and activity recognition method with signals, J. Supercomput. 76 (2020) 2119–2138.
[48] E. Aydemir, T. Tuncer, S. Dogan, A Tunable-Q wavelet transform and quadruple symmetric pattern based EEG signal classification method, Med. Hypotheses 134 (2020) 109519.